

# Luminescence Mechanisms in $\text{Eu}^{3+}$ -Activated $\text{BaAl}_2\text{B}_4\text{O}_{10}$ for Solid-State Lighting Applications

R. S. Palaspagar, S. R. Khandekar

Department of Physics, Shivramji Moghe Mahavidyalaya, Kelapur (Pandharkawada), Dist. Yavatmal (M.S.), INDIA.  
Department of Chemistry, Indira Mahavidyalaya, Kalamb, Dist. Yavatmal (M.S.), INDIA.

**ABSTRACT:** Red-emitting  $\text{Eu}^{3+}$ -activated  $\text{BaAl}_{2(0.98)}\text{B}_4\text{O}_{10:0.02}\text{Eu}^{3+}$  phosphors were successfully synthesized via the solution combustion route. The phase purity of the resulting material was confirmed through powder X-ray diffraction (XRD) analysis. Following synthesis and structural characterization, the photoluminescence behavior of the phosphors was examined at room temperature using a spectrofluorometer. The excitation spectrum displayed a broad absorption band spanning 200–400 nm, while emission peaks were detected at 580 nm, 591 nm, and 615 nm, corresponding to the  $^5\text{D}_0 \rightarrow ^7\text{F}_j$  ( $j = 0, 1, 2$ ) transitions under 238 nm excitation. These optical features indicate that  $\text{BaAl}_2\text{B}_4\text{O}_{10}:\text{Eu}^{3+}$  is a promising red-emitting phosphor, offering potential as a novel luminescent material for UV-excited solid-state lighting applications.

**KEY WORDS:** Alumino-Borate, Combustion synthesis, Photoluminescence.

## I. INTRODUCTION

Solid-state lighting (SSL) technologies increasingly rely on phosphor-converted LEDs to produce high-quality visible light with tailored color rendering and high luminous efficacy. Efficient UV-excited red phosphors are key components for near-ultraviolet LED (n-UV LED) architectures in which a UV chip pumps separate blue/green/red phosphors to produce white light or display primaries. Among inorganic host families, borates and alumino-borates have emerged as versatile matrices for rare-earth activators because of their structural diversity, relatively wide bandgaps, and favorable phonon spectra, which together reduce non-radiative losses and support narrow, intense 4f-line emissions [1].

Europium(III) remains the activator of choice for red emission due to its well-defined intra-4f transitions (notably  $^5\text{D}_0 \rightarrow ^7\text{F}_2$  near 615 nm), high color purity, and generally good thermal behaviour in many oxide and borate hosts. The hypersensitive electric dipole  $^5\text{D}_0 \rightarrow ^7\text{F}_2$  transition is sensitive to local site symmetry and covalency; therefore, host selection and site occupancy strongly influence emission intensity, spectral shape, and color coordinates. The charge-transfer band (CTB) that arises from  $\text{O}^{2-} \rightarrow \text{Eu}^{3+}$  transitions typically lies in the UV region (200–300 nm) in many oxide and borate lattices and provides an efficient route to populate  $\text{Eu}^{3+}$  emissive states under UV excitation [2].

Solution combustion synthesis (SCS) is a rapid and energy-efficient method for preparing oxide and borate phosphors. The method yields fine, porous powders with high surface area and often requires lower calcination temperatures than conventional solid-state routes; the high local temperatures during combustion promote phase formation and dopant incorporation. Systematic studies show that SCS processing parameters (fuel type and ratio, metal-nitrate-to-fuel stoichiometry, heating profile) strongly affect crystallinity, particle size, defect concentrations and ultimately optical performance. Using SCS to produce  $\text{Eu}^{3+}$ -doped borate materials is therefore attractive for scalable manufacture of phosphors [3].

Although  $\text{Eu}^{3+}$  activation of many borate hosts (Ba- and Bi-containing borates, aluminoborates, etc.) has been widely reported,  $\text{BaAl}_2\text{B}_4\text{O}_{10}$  (an alumino-borate with monoclinic symmetry) has not been comprehensively studied as an  $\text{Eu}^{3+}$  host in the literature to the authors' knowledge. Closely related barium-based borates (e.g.,  $\text{BaBi}_2\text{B}_4\text{O}_{10}:\text{Eu}^{3+}$ ) have shown promising red emission and color coordinates approaching NTSC red standards, indicating that the Ba-based 2:4:10 frameworks can produce high color-purity red phosphors. Systematic study of  $\text{Eu}^{3+}$  doped  $\text{BaAl}_2\text{B}_4\text{O}_{10}$  will therefore determine whether this host similarly supports efficient 615 nm emission and good chromaticity for SSL applications [4]. In this work, we synthesize  $\text{BaAl}_{2(1-x)}\text{B}_4\text{O}_{10:x}\text{Eu}^{3+}$  ( $x = 0.00\text{--}0.06$  mol fraction; optimized at  $x = 0.02$ ) using solution combustion, followed by controlled annealing. We present phase analysis (XRD), room-temperature photoluminescence excitation and emission (PLE/PL) data, CIE chromaticity coordinates, and a discussion of site symmetry, CTB contribution, and relative emission intensities. We benchmark the optical performance against recent high-color-purity  $\text{Eu}^{3+}$ -activated borates and assess potential for integration into n-UV-based LED devices.

## II. MATERIALS AND METHOD

The powder samples of  $\text{Eu}^{3+}$  activated  $\text{BaAl}_2\text{B}_4\text{O}_{10}$  (BABO) phosphor was prepared by a solution combustion technique. In our previous work, many borate host materials were successfully synthesized using this technique [5-7]. The stoichiometric amounts of high purity starting materials,  $\text{Ba}(\text{NO}_3)_2$  (A.R.),  $\text{Al}(\text{NO}_3)_3 \cdot 9\text{H}_2\text{O}$  (A.R.),  $\text{Eu}_2\text{O}_3$  (high purity 99.9%),  $\text{H}_3\text{BO}_3$  (A.R.),  $\text{CO}(\text{NH}_2)_2$  (A.R.) have been used for phosphors preparation. The stoichiometric amounts of the ingredients were thoroughly mixed in an Agate Mortar with adding little amount of double distilled water. The materials then transferred into china basin and heated on heating menthol at about  $70^\circ\text{C}$  so as to obtained clear solution. The solution was then introduced into a pre-heated muffle furnace maintained at temperature  $550^\circ\text{C}$  for combustion. The solution boils; foams and ignites to burn with flame which gave a voluminous, foamy powder. Following the combustion, the resulting foamy samples were crushed to obtain fine particles and then annealed in a slightly reducing atmosphere provided by burning charcoal at temperature  $750^\circ\text{C}$  for 2 hr and suddenly cooled to room temperature. The prepared materials were characterized by powder XRD. Powder X-ray diffraction measurements were taken on Rigaku Miniflex II X-ray Diffractometer and compared with the ICDD files. PL & PLE measurements at room temperature were performed on Hitachi F-7000 spectrofluorometer with spectral resolution of 2.5 nm.

## III. RESULTS AND DISCUSSION

### X-ray Diffraction Pattern

The X-ray diffraction (XRD) technique have been used to identify the phase composition, structure and their crystallinity with  $\text{CuK}\alpha$  radiation ( $\lambda = 1.5418 \text{ \AA}$ ). Figure 1 shows the XRD pattern of  $\text{BaAl}_{2(0.98)}\text{B}_4\text{O}_{10:0.02}\text{Eu}^{3+}$  phosphor. The XRD-pattern of the as prepared phosphor powder shows good agreement with standard ICDD File no.00-080-0109. The phosphor has monoclinic crystal structure with cell parameter  $a=12.709 \text{ \AA}$ ,  $b=9.432 \text{ \AA}$ ,  $c=5.621 \text{ \AA}$ . Here we first time prepared the compositions of the host materials by solution combustion methods.

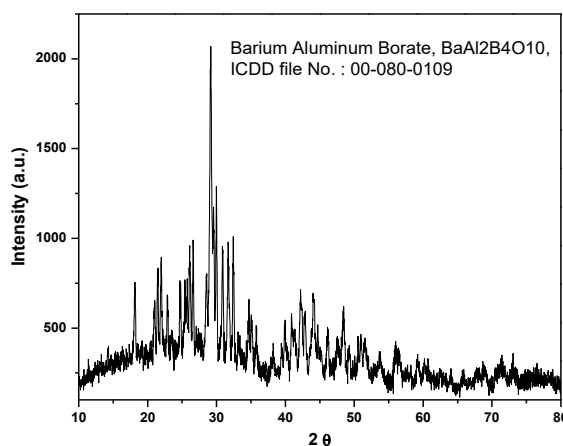


**Figure 1.** X-ray powder diffraction pattern of  $\text{BaAl}_2\text{B}_4\text{O}_{10}$  host phosphor.

### FE-SEM micrographs of phosphor powders

The FE-SEM photographs of  $\text{BaAl}_{2(0.98)}\text{B}_4\text{O}_{10:0.02}\text{Eu}^{3+}$  powders prepared by solution combustion method is shown in Figure 2. The shapes of the particles were observed to be random in nature with agglomeration for both the phosphors. The crystalline size of both the phosphors was observed to be varied in the range  $0.3\text{--}2 \mu\text{m}$ .

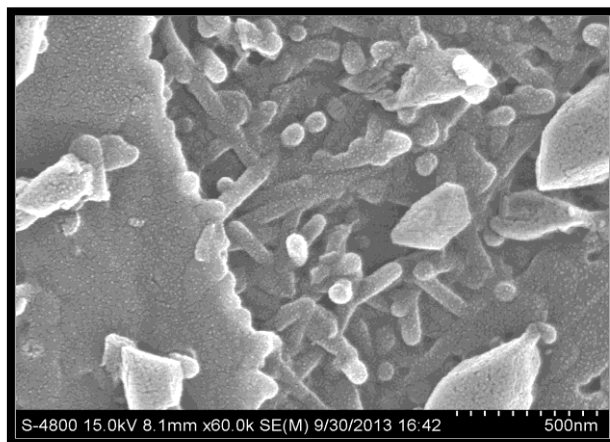


**Figure 2.** FE-SEM images of  $\text{BaAl}_2\text{B}_4\text{O}_{10}$ .

#### Photoluminescence of $\text{BaAl}_2\text{B}_4\text{O}_{10}:\text{Eu}^{3+}$

The photoluminescence (PL) and photoluminescence excitation (PLE) spectra of the  $\text{BaAl}_{2(0.98)}\text{B}_4\text{O}_{10:0.02}\text{Eu}^{3+}$  phosphors were recorded at room temperature. The typical excitation spectrum monitored at  $\lambda_{\text{em}} = 615 \text{ nm}$  and emission spectrum monitored at  $\lambda_{\text{ex}} = 238 \text{ nm}$  is as shown in Figure 3. The excitation spectra consist of sharp f-f transition lines in the wavelength range 300 nm to 400 nm, including  ${}^7\text{F}_0 \rightarrow {}^5\text{H}_3$  (320 nm),  ${}^7\text{F}_0 \rightarrow {}^5\text{D}_4$  (363 nm),  ${}^7\text{F}_0 \rightarrow {}^5\text{L}_7$  (383 nm) and  ${}^7\text{F}_0 \rightarrow {}^5\text{L}_6$  (393 nm). It is also observed that a broad excitation band in the wavelength range 200–300 nm, which can be attributed to the charge transfer from  $\text{O}^{2-}$  to  $\text{Eu}^{3+}$ , generally occurring between 200 and 300 nm. The charge transfer from  $\text{O}^{2-}$  to  $\text{Eu}^{3+}$  in  $\text{BaAl}_2\text{B}_4\text{O}_{10}$  lattices is observed stronger than sharp f-f transition lines. It is explained that  $\text{Eu}^{3+}$  ion replaces the  $\text{Al}^{3+}$  ion in the lattice but some of europium ion replaces the lithium ion in the lattice and some kind of defects (oxygen interstitials or displacement) has to be introduced to compensate for the charge in change. The emission spectrum depicts the typical red photoluminescence at 615 nm under the excitation at 393 and 238 nm. The emission spectrum consists of a series of sharp bands at 580 nm ( ${}^5\text{D}_0 \rightarrow {}^7\text{F}_0$ ), 591 nm ( ${}^5\text{D}_0 \rightarrow {}^7\text{F}_1$ ) and 615 nm ( ${}^5\text{D}_0 \rightarrow {}^7\text{F}_2$ ). In particular, the most intense emission peak at 615 nm occurs through the forced electric dipole while the  ${}^5\text{D}_0 \rightarrow {}^7\text{F}_1$  band at of  $\text{BaAl}_{2(1-x)}\text{B}_4\text{O}_{10:x}\text{Eu}^{3+}$  ( $x = 2\text{mole } \%$ ). 591 nm is due to the magnetic dipole transition as shown in figure 4.

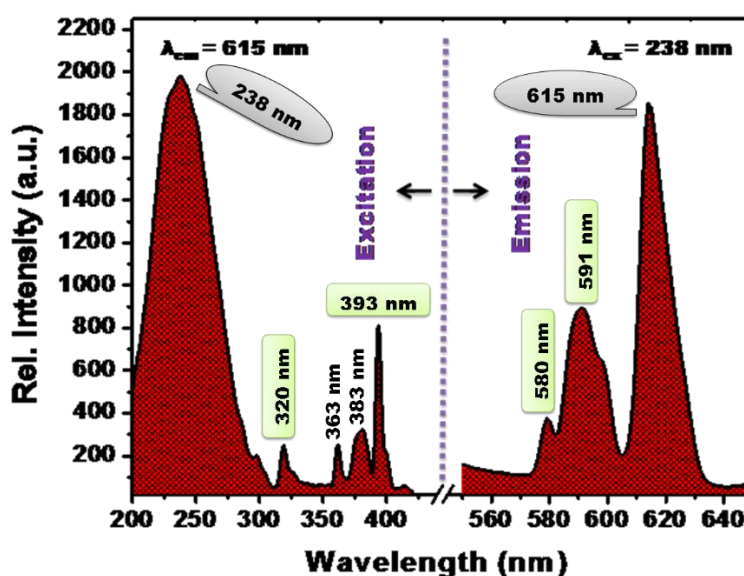


**Figure 3.** Excitation and emission spectra of  $\text{BaAl}_{2(0.98)}\text{B}_4\text{O}_{10:0.02}\text{Eu}^{3+}$  phosphor.

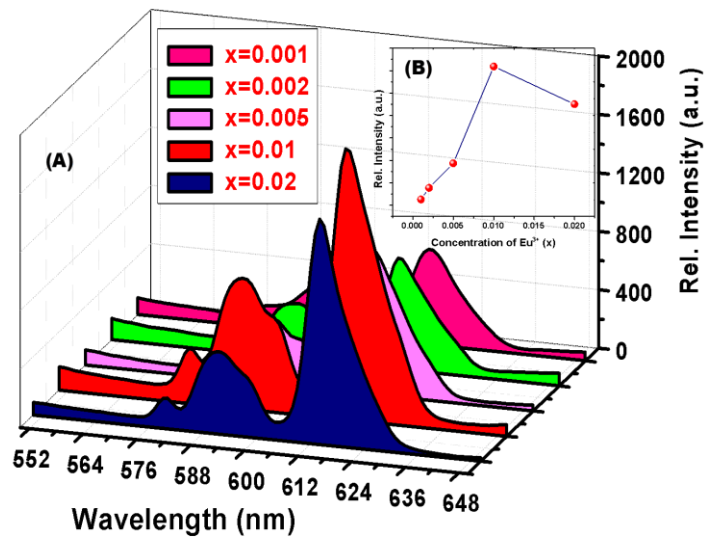


**Figure 4.** (A) Dependence of the PL intensities of  $\text{BaAl}_{2(0.98)}\text{B}_4\text{O}_{10:0.02}\text{Eu}^{3+}$  at  $\lambda_{\text{ex}}=238$  nm at different  $\text{Eu}^{3+}$  concentrations. (B) The top inset shows the influence of the concentration on the emission intensity of  $\text{BaAl}_{2(0.98)}\text{B}_4\text{O}_{10:0.02}\text{Eu}^{3+}$  phosphor (x=0.001, 0.002, 0.005, 0.01, and 0.02).

#### Colorimetry and application relevance

CIE coordinates for the emission centered at 615 nm were measured at (x = 0.68, y = 0.32), locating the emission circularly within the red region and comparable to other high color-purity  $\text{Eu}^{3+}$  borate phosphors as shown in figure 5. This chromaticity suggests suitability for n-UV-pumped devices where a deep red component is required. For device-level assessment, report PLQY under 393 nm and 238 nm excitation and combine  $\text{BABO}:\text{Eu}^{3+}$  with complementary green/blue phosphors to compute lamp-level CRI and correlated color temperature (CCT). Comparable hosts (e.g.,  $\text{BaBi}_2\text{B}_4\text{O}_{10}:\text{Eu}^{3+}$ ) have shown NTSC-like red coordinates, reinforcing the promise of Ba-based 2:4:10 systems [8].

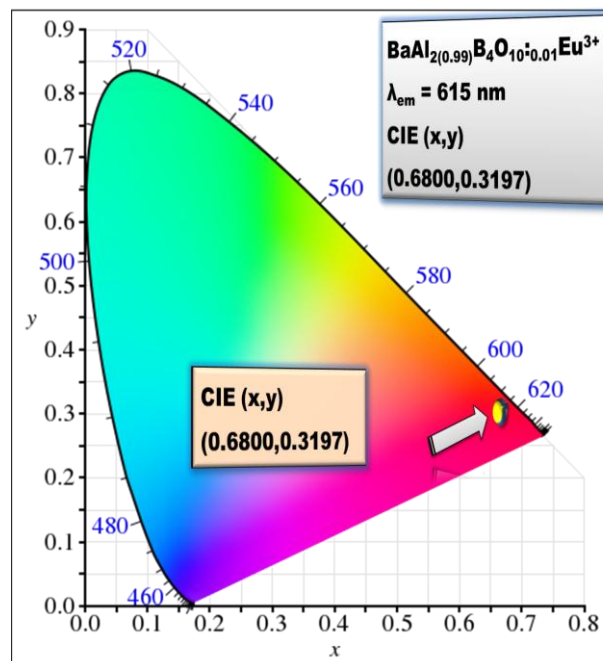


**Figure 5.** Chromaticity coordinates of  $\text{BaAl}_{2(0.98)}\text{B}_4\text{O}_{10:0.02}\text{Eu}^{3+}$  phosphor in the CIE 1931 chromaticity diagram.

### III. CONCLUSION

The phosphor  $\text{BaAl}_{2(0.98)}\text{B}_4\text{O}_{10:0.02}\text{Eu}^{3+}$  have been successfully synthesized by using a simple, time saving and cost effective solution combustion technique. The as synthesized phosphor shows strong emission band located at 615 nm corresponding to the  $^5\text{D}_0 \rightarrow ^7\text{F}_2$  transition spectra region originated from the transition of  $\text{Eu}^{3+}$  by keeping the excitation wavelength constant at 238 nm. The presence of a strong  $\text{O}^{2-} \rightarrow \text{Eu}^{3+}$  charge-transfer band and intense 4f emission indicate efficient UV-to-red conversion suitable for n-UV-LED pumped solid-state lighting. Therefore,  $\text{BaAl}_{2(0.98)}\text{B}_4\text{O}_{10:0.02}\text{Eu}^{3+}$  phosphors could be systematically used for generating the red light under UV radiation which may be promising candidates for solid-state lighting.

### REFERENCES

1. R.T. Maske, A.N. Yerpude, R.S. Wandhare, Amol Nande, S.J. Dhoble, Combustion synthesized novel  $\text{SrAlBO}_4:\text{Eu}^{3+}$  phosphor: Structural, luminescence, and Judd-Ofelt analysis, *Optical Materials*, Volume 141, 2023, 113893.
2. M. Kaczkan, M. Kowalczyk, S. Szostak, A. Majchrowski, M. Malinowski, Transition intensity analysis and emission properties of  $\text{Eu}^{3+}:\text{Bi}_2\text{ZnOB}_2\text{O}_6$  acentric biaxial single crystal, *Optical Materials*, Volume 107, 2020, 110045, ISSN 0925-3467.
3. Fizza Siddique, Sergio Gonzalez-Cortes, Amir Mirzaei, Tiancun Xiao, M. A. Rafiq and Xiaoming Zhang, Solution combustion synthesis: the relevant metrics for producing advanced and nanostructured photocatalysts, *RSC, Nanoscale*, 2022, 14, 11806-11868.
4. Shablinskii, A. P., Povolotskiy, A. V., Yuriev, A. A., Biryukov, Y. P., Bubnova, R. S., Avdontceva, M. S., Janson, S. Y., & Filatov, S. K. (2023). Novel Red-Emitting  $\text{BaBi}_2\text{B}_4\text{O}_{10}:\text{Eu}^{3+}$  Phosphors: Synthesis, Crystal Structure and Luminescence. *Symmetry*, 15(4), 918.
5. R.S. Palaspagar, A.B. Gawande, R.P. Sonekar, S.K. Omanwar, Combustion synthesis and photoluminescence properties of a novel  $\text{Eu}^{3+}$  doped lithium alumino-borate phosphor, *J. Lumin.*, 154 (2014) 58-61.
6. R.S. Palaspagar, A.B. Gawande, R.P. Sonekar, S.K. Omanwar, Fluorescence properties of  $\text{Tb}^{3+}$  and  $\text{Sm}^{3+}$  activated novel  $\text{LiAl}_7\text{B}_4\text{O}_{17}$  host via solution combustion synthesis, *Mater. Res. Bull.*, 72 (2015) 215-219.
7. R.S. Palaspagar, R.P. Sonekar, S.K. Omanwar, Fluorescence properties and energy transfer investigation of novel  $\text{Li}_2\text{Al}_2\text{B}_2\text{O}_7:\text{Ce}^{3+}$ ,  $\text{Tb}^{3+}$  phosphors via combustion synthesis, *J. Mater. Sci. Mater. Electron.*, 27(5), (2016) 4951.
8. Shablinskii, A. P., Povolotskiy, A. V., Yuriev, A. A., Biryukov, Y. P., Bubnova, R. S., Avdontceva, M. S., Janson, S. Y., & Filatov, S. K. (2023). Novel Red-Emitting  $\text{BaBi}_2\text{B}_4\text{O}_{10}:\text{Eu}^{3+}$  Phosphors: Synthesis, Crystal Structure and Luminescence. *Symmetry*, 15(4), 918.

### AUTHOR'S BIOGRAPHY

<b>Full name</b>	<b>Ritesh Shalikrao Palaspagar</b>
<b>Science degree</b>	M.Sc., Ph.D.
<b>Academic rank</b>	Assistant Professor
<b>Institution</b>	Shivramji Moghe Arts, Commerce & Science College.

<b>Full name</b>	<b>Snehal Ramrao Khandekar</b>
<b>Science degree</b>	M.Sc., NET
<b>Academic rank</b>	Assistant Professor
<b>Institution</b>	Indira Mahavidyalaya.